

## Research

### Two-Phase Mixture Numerical Study of Nanofluid Flow in a Lithium-Ion Battery Cooling System

Estudio numérico de mezcla bifásica del flujo de nanofluidos en un sistema de enfriamiento para una batería de iones de litio

Amina Benabderrahmane<sup>1</sup>  and Samir Laouedj<sup>2</sup>

<sup>1</sup> University of Mustapha Stambouli  (Mascara, Algeria)

<sup>2</sup> University Djilali Liabes  (Sidi bel abbes, Algeria).

#### Abstract

**Context:** The cooling performance of a thermal battery plays a critical role in its efficiency, lifespan, and safety. This importance stems from the heat generated during charging and discharging processes. As temperatures rise, key battery characteristics are significantly affected.

**Method:** Using the ANSYS Fluent computational fluid dynamics software, a 2D numerical simulation was conducted to study the cooling of a lithium-ion battery in the presence of nanofluids. The flow of nanofluids was analyzed using the multiphase mixture model.

**Results:** It was found that the coolant inlet velocity significantly impacts the module's temperature distribution and the maximum temperature difference, where the temperature differences almost stabilize for inlet velocities exceeding 0.3 m/s. The effect of using nanofluids was studied with three different types of nanoparticles (alumina, copper, and fullerene) dispersed in water as the base fluid. The results show that the temperature difference in the module varies depending on the nature and volume fraction of the nanoparticles. The incorporation of nanofluids leads to a significant reduction in module temperatures. Fullerene nanoparticles were found to exhibit superior cooling performance compared to other nanoparticle types. On the other hand, a nanoparticle volume fraction exceeding 2 % yields a nearly uniform temperature distribution within the module, as well as reduced cell temperatures.

**Conclusions:** Nanofluids have an important effect on battery cooling. Optimizing nanoparticle concentration and flow dynamics can effectively improve thermal management strategies for lithium-ion battery systems.

**Keywords:** computational fluid dynamics, lithium-ion battery, cooling, nanofluids, mixture, battery thermal management

#### Article history

**Received:**  
Oct 24<sup>th</sup>, 2024


**Modified:**  
Jun 16<sup>th</sup>, 2025

**Accepted:**  
Sep 1<sup>st</sup>, 2025

*Ing*, vol. 30, no. 2,  
2025, e22822

©The authors;  
reproduction right  
holder Universidad  
Distrital Francisco  
José de Caldas.



\*  **Correspondence:** [amina.benabderrahmane@univ-mascara.dz](mailto:amina.benabderrahmane@univ-mascara.dz)

Resumen

**Contexto:** El rendimiento de refrigeración de una batería térmica desempeña un papel fundamental en su eficiencia, vida útil y seguridad. Esta importancia se debe al calor generado durante los procesos de carga y descarga. A medida que aumentan las temperaturas, las características clave de la batería se ven significativamente afectadas.

**Método:** Utilizando el *software* de dinámica de fluidos computacional ANSYS Fluent, se realizó una simulación numérica 2D para estudiar el enfriamiento de una batería de iones de litio en presencia de nanofluidos. El flujo de nanofluidos se analizó utilizando el modelo de mezcla multifásica.

**Resultados:** Se observó que la velocidad de entrada del refrigerante afecta significativamente la distribución de temperatura del módulo y la diferencia máxima de temperatura, donde las diferencias de temperatura prácticamente se estabilizan para velocidades de entrada superiores a 0.3 m/s. Se estudió el efecto del uso de nanofluidos con tres tipos diferentes de nanopartículas (alúmina, cobre y fullereno) dispersas en agua como fluido base. Los resultados muestran que la diferencia de temperatura en el módulo varía según la naturaleza y la fracción de volumen de las nanopartículas. La incorporación de nanofluidos produce una reducción significativa en la temperatura del módulo. Se observó que las nanopartículas de fullereno presentan un rendimiento de refrigeración superior al de otros tipos de nanopartículas. Por otro lado, una fracción de volumen de nanopartículas superior al 2 % da como resultado una distribución de temperatura prácticamente uniforme dentro del módulo, así como una reducción en la temperatura de la celda.

**Conclusiones:** Los nanofluidos tienen un efecto importante en la refrigeración de las baterías. Optimizar la concentración de nanopartículas y la dinámica del flujo puede mejorar eficazmente las estrategias de gestión térmica de los sistemas de baterías de iones de litio.

**Palabras clave:** dinámica de fluidos computacional, batería de iones de litio, refrigeración, nanofluidos, mezcla, gestión térmica de la batería.

Table of contents

		<b>6. Results and interpretations</b>	<b>9</b>
		6.1. Effect of velocity inlet on cell temperature distribution . . . . .	9
		6.2. Effect of nanofluids on temperature distribution . . . . .	9
		6.3. Effect of nanofluids on heat transfer	11
		6.4. Effect of nanoparticle volume fraction on temperature distribution	13
<b>1. Introduction</b>	<b>3</b>	<b>7. Conclusion</b>	<b>15</b>
<b>2. Physical model</b>	<b>5</b>	<b>8. Author contributions</b>	<b>16</b>
<b>3. Boundary conditions</b>	<b>6</b>		
<b>4. Governing equations</b>	<b>7</b>		
<b>5. Mesh independence study</b>	<b>8</b>		

## Nomenclature

### Symbols

$C$	Specific heat, J/kg·K
$Nu$	Nusselt number
$p$	Pressure, Pa
$Q$	Heat
$Re$	Reynolds number
$T$	Temperature, K
$t$	Time, s
$V$	Velocity, m/s

### Greek Symbols

$\rho$	Density, kg/m <sup>3</sup>
$\mu$	Dynamic viscosity, Pa·s
$\lambda$	Thermal conductivity, W/m·K
$\phi$	Nanoparticles volume fraction

### Subscripts

$b$	Battery
$dr,k$	Drift velocity of the $k$ -th phases
$k$	Number of phases
$m$	Mixture
$p$	Particles
$w$	Water

### Acronyms

BTMS	Battery thermal management system
CFD	Computational fluid dynamics
CPCM	Composite phase change material
EV	Electrical vehicle
LIB	Lithium-ion battery
PCM	Phase change material
SOC	State of charge
TEC	Thermoelectric cooling

## 1. Introduction

Lithium-ion (Li-ion) batteries play an essential role in many modern applications, including electric vehicles, portable electronic devices, and renewable energy storage. The rapid development of this technology has led to a growing demand for efficient cooling systems to maintain batteries' optimum operating temperature. Inadequate battery cooling can lead to reduced efficiency, a shorter lifespan,

and even safety risks, such as overheating and fire. In response to these challenges, extensive research has focused on the use of nanofluids to improve battery cooling processes.

Most researchers have investigated the impact of improved heat transfer on battery performance through experimental, theoretical, and numerical studies. Experimental studies are frequently used to validate numerical results in practical cases, but they are generally more costly than other types of investigations.

(1) proposed an optimization method for the architecture of battery sensor systems based on an online sensing method to capture global electrothermal profiles in large-scale battery packs. Their results demonstrate that the double-layered technique can capture more information in a single step.

(2) experimentally studied the heat generation parameters of battery modules using three electrothermal models: Model A (constant resistance), Model B (resistance varying with depth of discharge), and Model C (resistance varying with both depth of discharge and temperature). They found that model C offers the best results for improving Li-ion battery performance and safety.

(3) numerically investigated the thermal performance of a battery thermal management system (BTMS) using phase change material (PCM) with three different mesh types. Their results demonstrated that the hexahedral mesh performs the closest to the experimental values.

(4) conducted a numerical investigation of the interaction between various fin configurations (namely sinusoidal and positive/negative straight fins) and local oscillation within a finned rectangular enclosure. They found that negative rectangular fins offer higher thermal performance, and that the effectiveness of oscillation decreases when localized between fins.

(5) examined the performance characteristics of Samsung li-ion batteries, *i.e.*, a INR21700 30T high-power (HP) cell and a INR21700 50E high-energy (HE) cell. According to their results, the HP cell had a greater rate capability, retaining 93.8 % of its capacity at 2C discharge, whereas the HE cell did the same at 1.6C.

In another work, the impact of using a thermoelectric cooler (TEC) to cool a Li-ion plate battery was numerically simulated using the COMSOL software (6). The heated part of the TEC was cooled by a heat sink, while the cold part was mounted on the battery. Three main types of heat sink were used. In addition, a non-Newtonian hybrid nanofluid served as the working fluid. For nanofluids with volume fractions of 0.05, 0.25, and 0.5 %, the heat sink temperature, the battery temperature, and the TEC's hot end temperature were calculated by varying the inlet Reynolds number (Re) between 200 and 800. The results showed that the application of Model C resulted in higher TEC temperatures. Models A and B kept the battery and heat sink temperatures low during periods of both low and high Re. As Re increased, the battery, TEC, and heat sink temperatures decreased, while the amount of  $\Delta P$  increased. The highest and lowest  $\Delta P$  values were found in Models C and A, respectively. The addition

of nanoparticles increased the  $\Delta P$  by 267 and  $\approx 95\%$  at  $Re = 200$  and  $800$ , respectively. (7) created electrochemical-thermal combination models for Li-ion cell modules arranged in series, investigating a unique mixed thermal management system comprising (PCM) and liquid cooling via a thermally conductive structure. The hybrid cooling system was initially tuned using this method, studying the impact of cell separation and incoming liquid velocity on electrical, chemical, and thermal efficiencies. As spacing increased, the highest temperature and the selection temperature difference decreased, but once the gap reached around  $4\text{ mm}$ , the rate of decrease almost disappeared. The main reason for the discharge imbalance between cells in the battery module was diffusion polarization in the electrolyte, which can be corrected by the proposed hybrid cooling system, according to a theoretical calculation used to assess and quantify unequal discharge.

(8) studied a liquid cooling BTMS for 18650 Li-ion batteries. Nanofluids with high thermal conductivity were used as coolants to improve thermal performance. Various nanofluids were compared against water in order to evaluate their cooling effectiveness. The best-performing solution was a Cu water-based nanofluid, which reduced the maximum temperature difference between the battery and the water by  $1.066\text{ K}$  and  $12.6\%$ , respectively. The results show that, although the volume percentage and the displacement velocity of the nanofluids increased simultaneously with the pressure drop, the maximum temperature difference and the maximum battery temperature decreased.

(9) investigated a dual cooling method combining forced convection cooling and convergent channels with composite phase-change material (CPCM). The results showed that, when hybrid cooling is used, the unit temperature drops below the safety limit. In addition, higher temperature uniformity and improved thermal performance are achieved when the CPCM surrounds the battery cell rather than being sandwiched between the cold plates and the battery cell.

Furthermore, a unique liquid cooling system, with stepped and zigzag channels consisting of alumina nanofluid and copper coating, was numerically investigated to improve the cooling capacity and temperature distribution of battery thermal control systems during discharge and charge processes (10). The results suggest that the maximum temperature and the temperature non-uniformity of the battery module were significantly reduced when a cooling alumina nanofluid with a volume fraction of  $2\%$  was added. Various studies using numerical, experimental, and mathematical methods have been conducted to examine the impact of different cooling systems and various coolants on the electrical and thermal performance of many engineering systems (11–26).

## 2. Physical model

A 2D numerical simulation was conducted in order to study the cooling of a Li-ion battery in the presence of nanofluids. This was done using the ANSYS Fluent computational fluid dynamics (CFD) software. The battery module consisted of 90 cylindrical Li-ion cells with nominal specifications of  $54\text{ V}/13.2\text{ Ah}$ . The cooling plates, made from aluminum, were sandwiched between two rows of cells. The gaps between two adjacent cells in the  $x$ - and  $y$ -axes measured  $2$  and  $4\text{ mm}$ , respectively, with air filling

the space between adjacent cells in the x-axis. A detailed schematic diagram of the battery module is shown in Fig. 1.

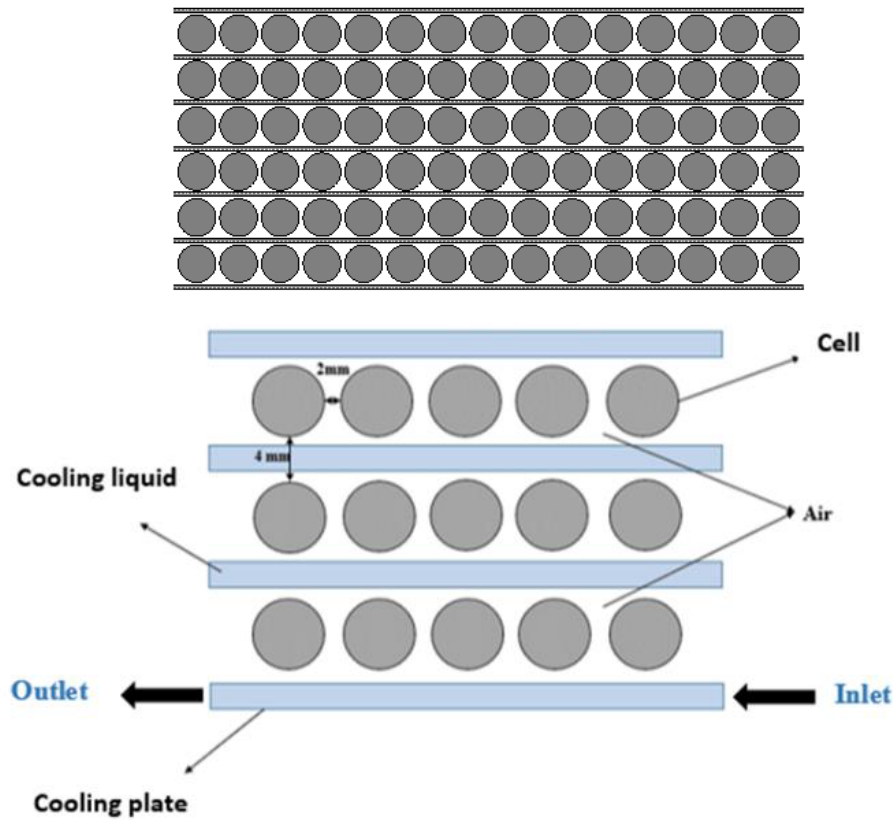


**Figure 1.** Schematic diagram of the battery module

The key technical specifications of an actual Li-ion battery cell typically include a nominal voltage of 3.7 V and a maximum voltage of around 4.2 V. The lowest voltage that the cell can reach before discharging becomes detrimental is usually around 3.0 V (27). The C-rate is commonly used to represent the charge/discharge rate. It is calculated by dividing the charge/discharge current by the nominal capacity. The cathode is constructed from a lithium cobalt oxide (LCO), and the anode is from graphite. A lithium salt dissolved in an ethylene carbonate is generally used as the electrolyte, which facilitates the movement of lithium ions between the electrodes during the operation of the battery. During discharge, lithium ions move from the anode to the cathode through the electrolyte, and, during charging, the process is reversed.

### 3. Boundary conditions

The boundary conditions for the inlet and outlet of the liquid cooling system were defined as the velocity inlet and the pressure outlet, respectively (Fig. 1). All surfaces inside the battery module were set as adiabatic boundary conditions. The initial liquid inlet and cell temperatures were set at 25 and 31 °C. The flow was considered to be laminar. In all studies, the Reynolds number was set between 700

and 1800. Three type of nanoparticles were employed in this work: alumina, copper, and fullerene. The thermophysical properties of the materials and nanoparticles are shown in Tables I and II.

**Table I.** Thermo-physical properties of the battery module materials (27)

	$\rho$ (kg/m <sup>3</sup> )	$C_p$ (J/ kg K)	$\lambda$ (W /mk)
Aluminum	2719	871	202.4
Lithium-ion	2904	894	1.035

**Table II.** Thermo-physical properties of nanoparticles used (28,29)

Nanoparticles	$\rho$ (kg/m <sup>3</sup> )	$C_p$ (J/ kg K)	$\lambda$ (W /mk)
Al <sub>2</sub> O <sub>3</sub>	3970	765	40
Cu	8954	385	401
C	3500	509	2300

## 4. Governing equations

The energy conservation equations for the cell (battery) and liquid coolant (water) are presented below (30).

$$\rho_b C_b \frac{\partial T}{\partial t} = \nabla \cdot (\lambda_b \nabla T) + \dot{Q} \quad (1)$$

$$\rho_w C_w \frac{\partial T_w}{\partial t} = \nabla \cdot (\lambda_b \nabla T_w) - \nabla \cdot (\rho_w C_w \vec{v} T_w) \quad (2)$$

The equations for the conservation of mass and the momentum of liquid cooling are as follows (31):

$$\frac{d\rho_w}{dt} + \nabla \cdot (\rho_w \vec{v}) = 0 \quad (3)$$

$$\frac{d}{dt}(\rho_w \vec{v}) + \nabla \cdot (\rho_w \vec{v} \vec{v}) = -\nabla p \quad (4)$$

For nanofluid flow simulation, we opted for the mixture two-phase model. The equations governing the flow are presented below (32).

$$\nabla \cdot (\rho_m \vec{V}_m) = 0 \quad (5)$$

$$\nabla \cdot \left( \sum_{k=1}^n (\rho_k C_{pk} \phi_k V_k T) \right) = \nabla \cdot (k_m \nabla T) \quad (6)$$

$$\rho_m \vec{V}_m \nabla \vec{V}_m = -\nabla p_m + (\mu_m \nabla \vec{V}_m) + \rho_m + \nabla \cdot \left( \sum_{k=1}^n (\phi_k \rho_k \vec{V}_{dr,k} \vec{V}_{dr,k}) \right) \quad (7)$$

where the  $k$ -th phase's drift velocity is calculated as follows :

$$\vec{V}_{dr,k} = \vec{V}_k - \vec{V}_m \quad (8)$$

The mixture properties are defined below.

$$\text{Velocity: } \vec{V}_m = \frac{\sum_{k=1}^n \rho_k \phi_k \vec{V}_k}{\rho_m} \quad (9)$$

$$\text{Density: } \rho_m = \sum_{k=1}^n \rho_k \phi_k \quad (10)$$

$$\text{Viscosity: } \mu_m = \sum_{k=1}^n \phi_k \mu_k \quad (11)$$

## 5. Mesh independence study

To assess the influence of grid size on the calculations, a grid sensitivity study was conducted, varying the total number of grid distributions in the radial and axial directions. Various combinations of grids were analyzed to ensure that the numerical results were independent of the mesh size used. Table III shows the evolution of the average Nusselt number as a function of the number of cells for a range of Reynolds numbers between 710 and 1775. It was found that increasing the number of meshes does not change the solution but does require more computation time. In this case, we used a mesh with 447 095 cells, since this value is the best in terms of both accuracy and processing times. These results underscore the fundamental principles of fluid dynamics and heat transfer in battery thermal management. Maintaining optimal fluid velocities is crucial for achieving a uniform temperature distribution and enhancing the overall cooling performance. This physical understanding highlights the necessity of balancing flow dynamics with thermal requirements to optimize battery operation and longevity. In fact, better accuracy can be obtained by using grid sizes with more nodes, but increasing the density of the cells would in turn increase the computational burden.

**Table III.** Mesh independence study

	Cells number			$\varepsilon_{\max}$
	390210	447095	580043	
Re	Nu			
710	37.04	37.20	37.17	0.004
1065	47.19	47.95	48.02	0.017
1420	53.33	53.82	54.11	0.014
1775	77.12	77.45	77.78	0.008



## 6. Results and interpretations

### 6.1. Effect of velocity inlet on cell temperature distribution

This study focused on exploring how the fluid inlet velocity influences the cooling efficiency of the battery module. Four distinct inlet velocities (0.1, 0.2, 0.3, and 0.4 m/s) were examined under controlled inlet temperature and module conditions. Fig. 2 presents the temperature contours across the module after a rapid charging cycle at varying inlet velocities. Notably, when the inlet velocity is below 0.2 m/s, the temperature distribution within the module exhibits significant non-uniformity.

Figs. 3 and 4 present the module's peak temperature and maximum temperature differential ( $\Delta T_{\max}$ ) as a function of different inlet velocities. Initially, both metrics decrease sharply and stabilize around velocities exceeding 0.3 m/s. This implies that an inlet velocity of 0.3 m/s can adequately facilitate efficient cooling within this water cooling system.

These results underscore the fundamental principles of fluid dynamics and heat transfer in battery thermal management. Maintaining optimal fluid velocities is crucial for achieving a uniform temperature distribution and enhancing the overall cooling performance. This physical understanding highlights the necessity of balancing flow dynamics with thermal requirements to optimize battery operation and longevity.

### 6.2. Effect of nanofluids on temperature distribution

This study investigated the impact of using nanofluids as coolants. Three types of nanoparticles were employed: copper, alumina, and fullerene. We used a mixture model to simulate the two-phase flow of the nanofluids, with water as the primary phase and nanoparticles dispersed in the base liquid as the secondary phase.

Fig. 5 illustrates the evolution of the temperature difference within the module when nanoparticles are dispersed in water. The results demonstrate that nanofluids can effectively reduce module temperatures thanks to their significantly enhanced heat transfer, which is facilitated by their high thermal conductivity of nanoparticles, *i.e.*, the measure of a material's ability to conduct heat, which plays a crucial role in enhancing the heat dissipation capacity. Notably, the fullerene/water coolant exhibits superior performance, attributed to fullerene's exceptional thermophysical properties, including high thermal conductivity and heat capacity.

Figs. 6 to 9 depict the temperature contours across the module for four different coolants under identical conditions (an inlet temperature of 298 K, an inlet velocity of 0.3 m/s, and a nanoparticle volume fraction of 0.01). These findings underscore the physical mechanisms underlying nanofluid cooling, emphasizing the importance of nanoparticle selection and concentration in optimizing thermal management strategies for battery systems.

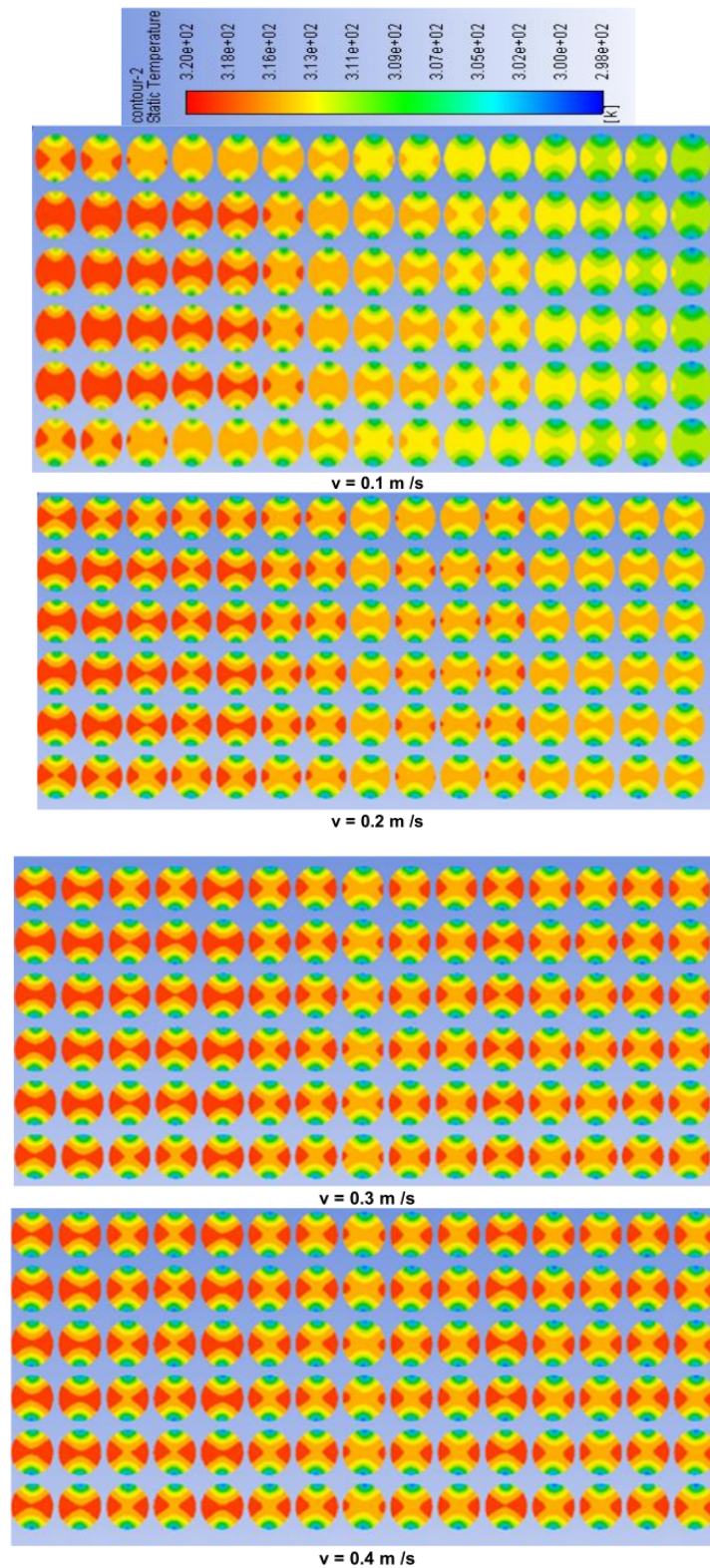


**Figure 2.** Module temperature contours for different inlet velocities

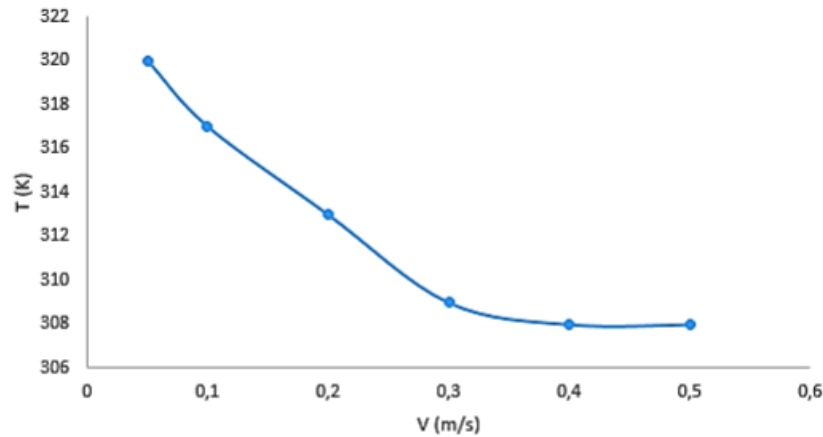


Figure 3.  $T_{\max}$  of the module as a function of the inlet velocity

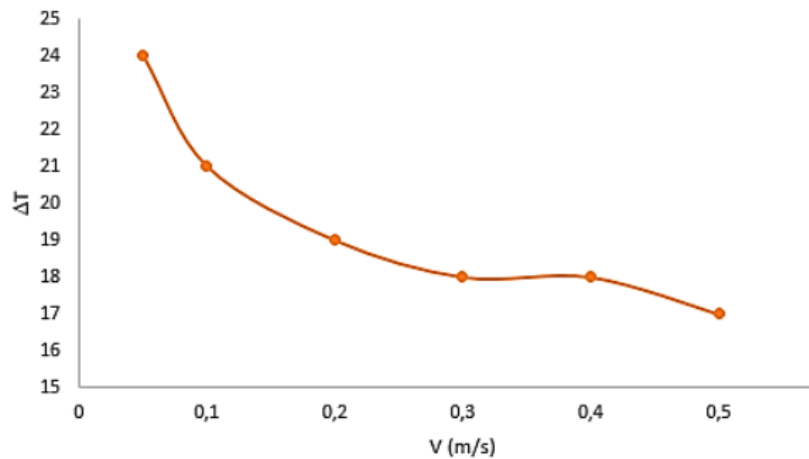


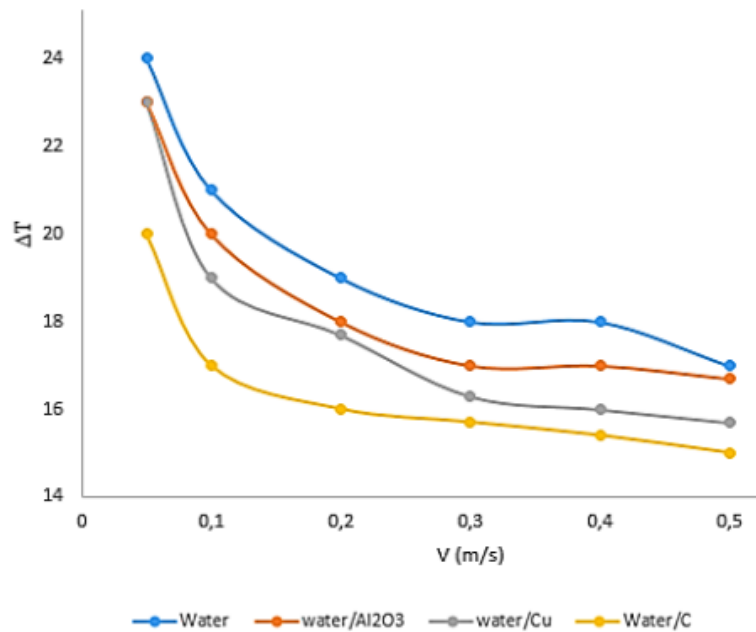
Figure 4.  $\Delta T_{\max}$  of the module as a function of the inlet velocity

### 6.3. Effect of nanofluids on heat transfer

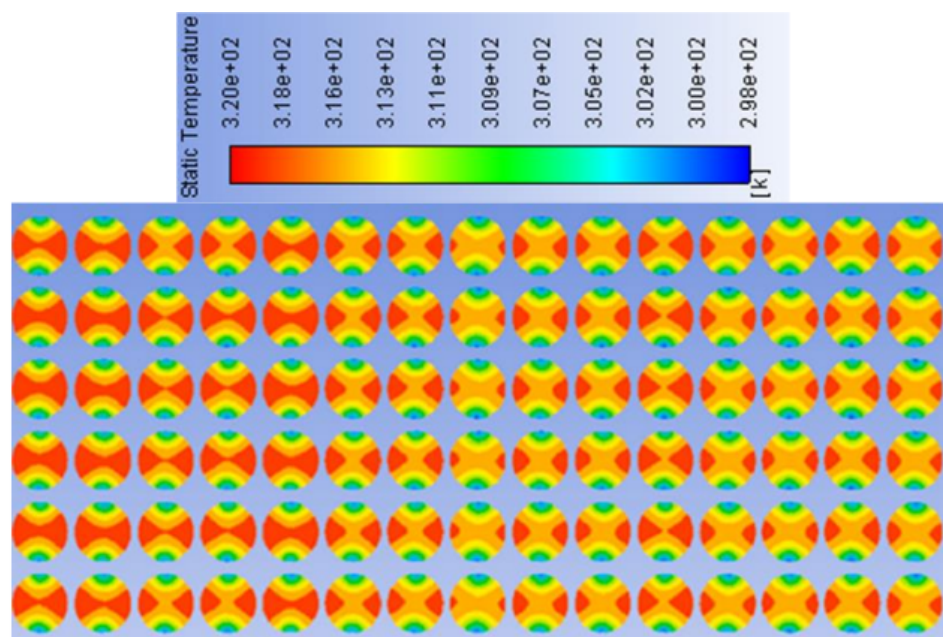
Fig. 10 demonstrates that the Nusselt number increases proportionally with the Reynolds number and is significantly influenced by the physical properties of the fluid utilized. Notably, the use of nanofluids shows a marked enhancement in this value.

Fig. 11 highlights that the highest Nusselt number was achieved with water/fullerene as the cooling fluid. This notable improvement can be attributed to the exceptional thermal conductivity of fullerene nanoparticles. Thermal conductivity plays a pivotal role in heat transfer efficiency, as it enables a faster dissipation of heat from the battery module. Fullerene's high thermal conductivity enhances convective heat transfer within the cooling system, leading to a more effective cooling performance.

These observations underscore the importance of nanoparticle selection and its impact on enhancing the thermal transport properties of nanofluid-based cooling systems. By optimizing fluid composition



**Figure 5.** Effect of nanofluids on the  $\Delta T_{\max}$  of the module as a function of the inlet velocity



**Figure 6.** Module temperature contours (cooling fluid: water)

and flow dynamics, engineers can effectively improve heat dissipation and enhance the overall thermal management of battery systems.



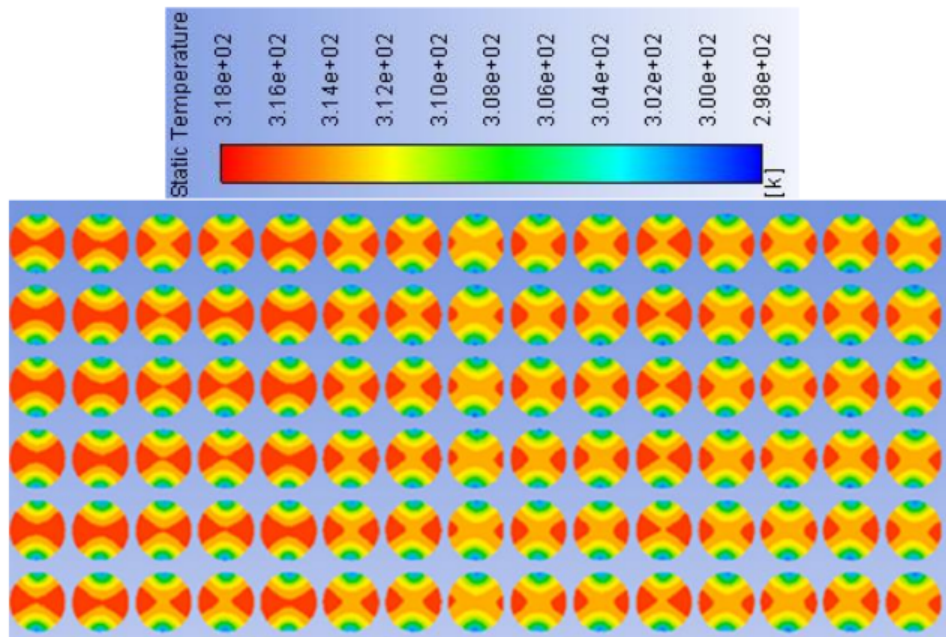


Figure 7. Module temperature contours (cooling fluid: water/ $\text{Al}_2\text{O}_3$ )

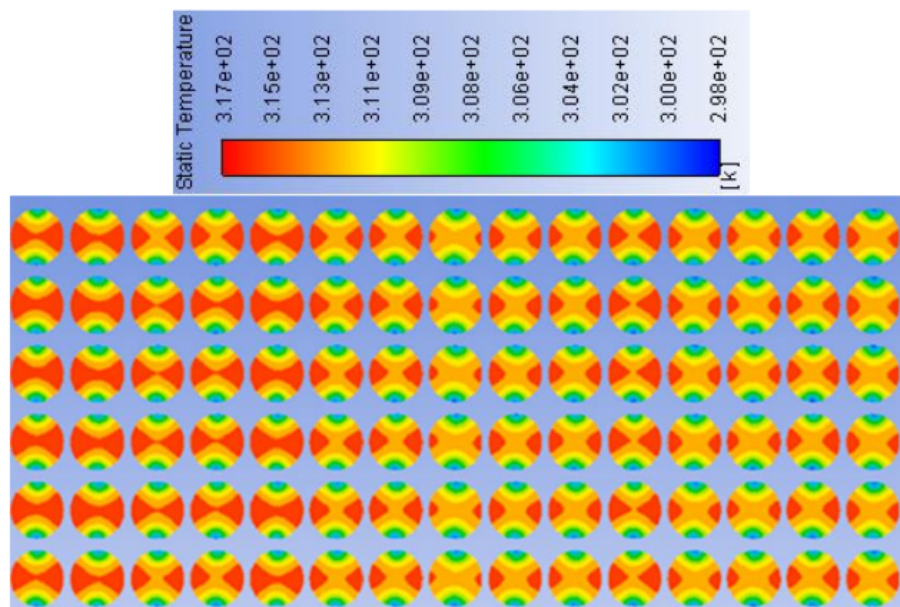


Figure 8. Module temperature contours (cooling fluid: water/ $\text{Cu}$ )

#### 6.4. Effect of nanoparticle volume fraction on temperature distribution

To investigate the impact of the fullerene nanoparticle volume fraction on the module's temperature distribution, the volume concentration was varied from 0.01 to 0.04. The results are depicted in Fig. 12, where it is evident that the temperature difference decreases with an increasing volume fraction. This reduction indicates that nanofluids effectively contribute to battery cooling.

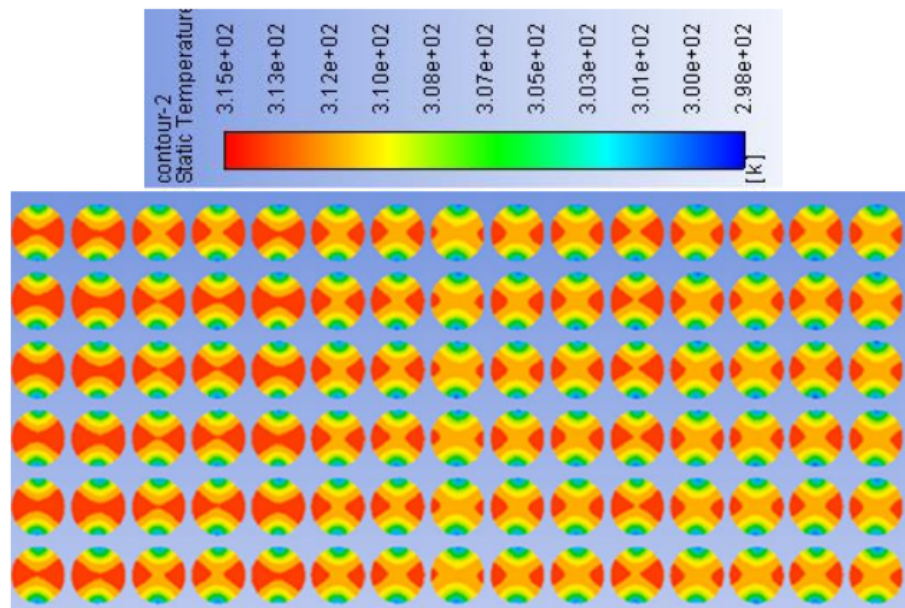


Figure 9. Module temperature contours (cooling fluid: water/C)

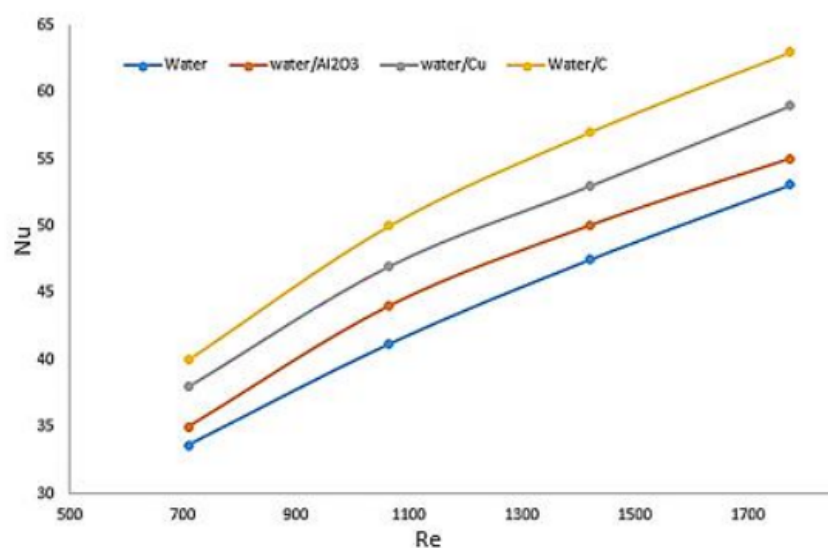
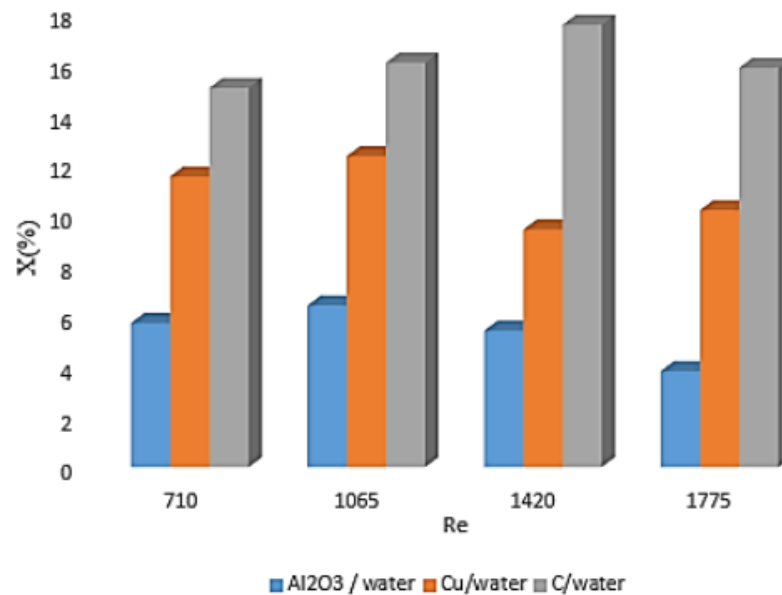
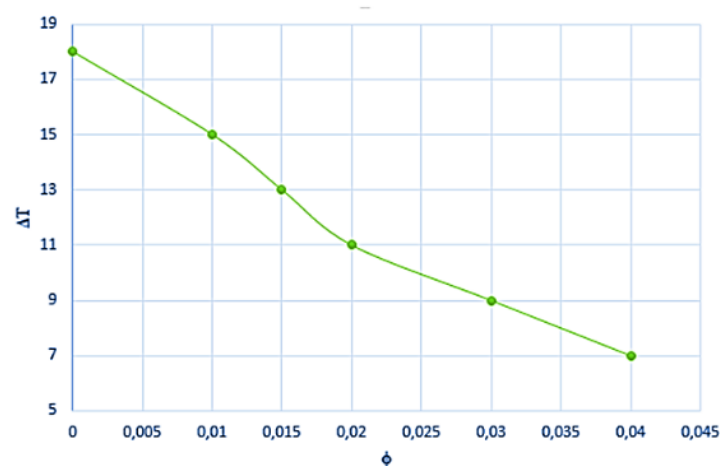


Figure 10. Effect on nanofluids on the Nusselt number as a function of the Reynolds number

It has been widely recognized in the industry that the optimal operating temperature range for Li-Ion Batteries is between 20 and 40 °C, with the temperature difference ( $\Delta T$ ) ideally controlled below 6 °C. Effective thermal management, facilitated by nanofluid cooling systems, plays a critical role in maintaining these temperature parameters within safe and efficient limits.



**Figure 11.** Rate of heat transfer improvement in the presence of nanofluids ( $\phi=0.01$ )



**Figure 12.** Variation in temperature difference as a function of the fullerene nanoparticle volume fraction ( $T_e=298\text{K}$ ,  $V=0.3\text{ m/s}$ )

## 7. Conclusion

In this work, a two-dimensional numerical study was conducted, with the aim of investigating the cooling of a Li-ion battery using nanofluids. We employed a stationary laminar regime and utilized the mixture multiphase model to simulate a two-phase flow. The key findings are summarized below.

- The temperature distribution within the battery module exhibits non-uniformity at inlet velocities below  $0.2\text{ m/s}$ .
- Temperature differences stabilize noticeably for inlet velocities exceeding  $0.3\text{ m/s}$ .

- The incorporation of nanofluids leads to significantly reduced module temperatures.
- Fullerene nanoparticles demonstrate superior cooling performance compared to other nanoparticle types.
- Achieving a nanoparticle volume fraction exceeding 2 % results in a nearly uniform temperature distribution within the module, as well as in reduced cell temperatures.

These results underscore the effectiveness of nanofluids in enhancing battery cooling efficiency, with fullerene nanoparticles proving particularly advantageous. Optimizing the nanoparticle concentration and flow dynamics can effectively improve thermal management strategies for Li-ion battery systems.

## 8. Author contributions

*Amina Benabderrahmane:* was mainly responsible for the development of the methodology, the implementation of the numerical model, and the collection and organization of the results. She also prepared the first draft of the manuscript.

*Samir Laouedj:* contributed to the conceptualization of the study and the validation of the results obtained. He supervised the research work, provided critical revisions to the manuscript, and ensured the scientific consistency of the paper.

## References

- [1] W. Li *et al.*, "A holistic electrothermal profiles online sensing method with sparse sensor system in large-format battery pack," *IEEE Trans. Ind. Elect.*, vol. 72, no. 10, pp. 10257-10266, 2025. <https://doi.org/10.1109/TIE.2025.3555004> ↑4
- [2] S. Vashisht, D. Rakshit, S. Panchal, M. Fowler, and R. Fraser, "Experimental estimation of heat generating parameters for battery module using inverse prediction method," *Int. Comm. Heat Mass Trans.*, vol. 162, art. 108539, 2025. <https://doi.org/10.1016/j.icheatmasstransfer.2024.108539> ↑4
- [3] E. Yousefi *et al.*, "Electrochemical-thermal modeling of phase change material battery thermal management systems: investigating mesh types for accurate simulations," *Int. J. Heat Mass Tran.*, vol. 247, art. 127107, 2025. <https://doi.org/10.1016/j.ijheatmasstransfer.2025.127107> ↑4
- [4] A. H. Vakilzadeh, A. B. Sarvestani, K. Javaherdeh, R. Kamali, and S. Panchal, "To what extent does local oscillation influence the thermal performance of finned PCM-based energy storage systems: A numerical study," *Int. J. Heat Fluid Flow*, vol. 114, art. 109798, 2025. <https://doi.org/10.1016/j.ijheatfluidflow.2025.109798> ↑4
- [5] Q. Yao, P. Kollmeyer, J. Chen, S. Panchal, O. Gross, and A. Emadi, "Study of high-power and high-energy lithium-ion batteries: From parameter analysis to physical modeling and experimental validation" SAE Technical Paper, 2025. [Online]. Available: <https://www.sae.org/publications/technical-papers/content/2025-01-8372/> ↑4



- [6] H. Alhumade, E. Almatrafi, M. Rawa, A. S. El-Shafay, C. Qi, and Y. Khetib, "Numerical study of simultaneous use of non-Newtonian hybrid nano-coolant and thermoelectric system in cooling of lithium-ion battery and changes in the flow geometry," *J. Power Sources*, vol. 540, art. 231626, 2022. <https://doi.org/10.1016/j.jpowsour.2022.231626> ↑4
- [7] Y. Yang *et al.*, "Thermal-electrical characteristics of lithium-ion battery module in series connection with a hybrid cooling," *Int. J. Heat Mass Tran.*, vol. 184, art. 122309, 2022. <https://doi.org/10.1016/j.ijheatmasstransfer.2021.122309> ↑5
- [8] G. Liao, W. Wang, F. Zhang, E. Jiaqiang, J. Chen, and E. Leng, "Thermal performance of lithium-ion battery thermal management system based on nanofluid," *Appl. Therm. Eng.*, vol. 216, art. 118997, 2022. <https://doi.org/10.1016/j.applthermaleng.2022.118997> ↑5
- [9] M. Faizan, S. Pati, and P. Randive, "Implications of novel cold plate design with hybrid cooling on thermal management of fast discharging lithium-ion battery," *J. Energy Storage*, vol. 53, art. 105051, 2022. <https://doi.org/10.1016/j.est.2022.105051> ↑5
- [10] A. Sarchami *et al.*, "A novel nanofluid cooling system for modular lithium-ion battery thermal management based on wavy/stair channels," *Int. J. Therm. Sci.*, vol. 182, art. 107823, 2022. <https://doi.org/10.1016/j.ijthermalsci.2022.107823> ↑5
- [11] K. Joshi, D. Dandotiya, C. S. Ramesh, and S. Panchal, "Numerical analysis of battery thermal management system using passive cooling technique," SAE Technical Paper, 2023. [Online]. Available: <https://doi.org/10.4271/2023-01-0990> ↑5
- [12] S. Panchal, V. Pierre, M. Cancian, O. Gross, F. Estefanous, and T. Badawy, "Development and validation of cycle and calendar aging model for 144Ah NMC/graphite battery at multi temperatures, DODs, and C-rates," SAE Technical Paper, 2023. [Online]. Available: <https://doi.org/10.4271/2023-01-0503> ↑5
- [13] H. A. Hasan, S. Jenan, M. A. Azher, S. S. Hakim, and K. Sopian, "Improve the performance of solar thermal collectors by varying the concentration and nanoparticles diameter of silicon dioxide, Open Engineering, vol. 12, no. 1, pp. 743–751, 2022. <https://doi.org/10.1515/eng-2022-0339> ↑5
- [14] K. A. Ameen, M. J. A. Hasan, Al-Dulaimi, A. M. Abed, and F. Haidar, "Improving the performance of air conditioning unit by using a hybrid technique," *MethodsX*, vol. 9, art. 101620, 2022. <https://doi.org/10.1016/j.mex.2022.101620> ↑5
- [15] W. Li *et al.*, "An internal heating strategy for lithium-ion batteries without lithium plating based on self-adaptive alternating current pulse," *IEEE Trans. Vehic. Tech.*, vol. 72, no. 5, pp. 5809–5823, 2022. <https://doi.org/10.1109/TVT.2022.3229187> ↑5
- [16] H. A. Hasan, S. S. Jenan, J. M. Mahdi, H. Togun, M. A. Azher, R. K. Ibrahim, and W. Yaïci, "Experimental evaluation of the thermoelectrical performance of photovoltaic-thermal systems with a water-cooled heat sink," *Sustainability*, vol. 14, no. 16, art. 10231, 2022. <https://doi.org/10.3390/su141610231> ↑5
- [17] R. Braga *et al.*, "Transient electrochemical model development and validation of a 144 Ah cell performance under different drive cycles conditions," SAE Technical Paper, 2023. [Online]. Available: <https://doi.org/10.4271/2023-01-0513> ↑5

- [18] N. S. Rukman *et al.*, "Bi-fluid cooling effect on electrical characteristics of flexible photovoltaic panel," *J. Mech. Electr. Power, and Veh. Tech.*, vol. 12, no. 1, pp. 51–56, 2021. <https://doi.org/10.14203/J.MEV.2021.V12.51-56> ↑5
- [19] C. Vivek, A. S. Dhoble, S. Panchal, D. Fowler, and D. Fraser, "Experimental and numerical investigation on thermal characteristics of 2×3 designed battery module," 2023. [Online]. Available: <https://dx.doi.org/10.2139/ssrn.4568465> ↑5
- [20] H. N. Khaboshan, F. Jaliliantabar, A. Abdullah, and S. Panchal, "Improving the cooling performance of cylindrical lithium-ion battery using three passive methods in a battery thermal management system," *Appl. Therm. Eng.*, vol. 227, art. 120320, 2023. <https://doi.org/10.1016/j.applthermaleng.2023.120320> ↑5
- [21] K. A. Ameen, M. J. Al-Dulaimi, H. A. Abraham, and H. A. Hasan, "Experimental study to increase the strength of the adhesive bond by increasing the surface area arrangement," *IOP Conf. Ser. Mater. Sci. Eng.*, vol. 765, pp. 1–10, 2020. <https://doi.org/10.1088/1757-899X/765/1/012054> ↑5
- [22] A. M. Aboghrara, B. T. H. T. Baharudin, M. A. Alghoul, N. M. Adam, A. A. Hairuddin, H. A. Hasan, "Performance analysis of solar air heater with jet impingement on corrugated absorber plate," *Case Stud. Therm. Eng.*, vol. 10, pp. 111–120, 2017. <https://doi.org/10.1016/j.csite.2017.04.002> ↑5
- [23] H. Abdulrasool, A. Ali, L. Abdulredh, and M. A. Azher, "Numerical investigation of nanofluids comprising different metal oxide nanoparticles for cooling concentration photovoltaic thermal CPVT," *Cleaner Eng. Tech.*, vol. 10, art. 100543, 2022. <https://doi.org/10.1016/j.clet.2022.100543> ↑5
- [24] H. Togun *et al.*, "Numerical simulation on heat transfer augmentation by using innovative hybrid ribs in a forward-facing contracting channel," *Symmetry*, vol. 15, no. 3, art. 690, 2023. <https://doi.org/10.3390/sym15030690> ↑5
- [25] A-dulaimi, J. Mustafa, H. H. Areej, H. A. Hasan, and F. A. Hamad, "Energy and exergy investigation of a solar air heater for different absorber plate configurations," *Int. J. Automot. Mech. Eng.*, vol. 20, no. 1, pp. 10258–10273, 2023. <https://journal.ump.edu.my/ijame/article/view/7317/2742> ↑5
- [26] A. Hasan, H. T. Husam, M. A. Azher, I. M. Hayder, and N. Biswas, "A novel air-cooled Li-ion battery (LIB) array thermal management system – a numerical analysis," *Int. J. Therm. Sci.*, vol. 190, art. 108327, 2023. <https://doi.org/10.1016/j.ijthermalsci.2023.108327> ↑5
- [27] M. Bahiraei, F. Nazri, and G. A. Saif, « Electrochemical-thermal model of pouch-type lithium-ion batteries," *Electrochimica Acta*, vol. 247, pp. 569–587, 2017. <http://dx.doi.org/10.1016/j.electacta.2017.06.164> ↑6,7
- [28] M. S. A. Kashkooli, F. M. Ghalambaz, and A. J. Chamkha, "Free convection of hybrid Al<sub>2</sub>O<sub>3</sub>-Cu water nanofluid in a differentially heated porous cavity," *Adv. Powder Tech.*, vol. 28, no. 9, pp. 2295–2305, 2017. <https://doi.org/10.1016/J.APT.2017.06.011> ↑7
- [29] Y. Pan *et al.*, "Advances in photocatalysis based on fullerene C<sub>60</sub> and its derivatives: Properties, mechanism, synthesis, and applications," *App. Catal. B Environ*, vol. 265, art. 118579, 2020. <https://doi.org/10.1016/j.apcatb.2019.118579> ↑7

- [30] Z. Rao, Z. Qian, Y. Kuang, and Y. Li, "Thermal performance of liquid cooling based thermal management system for cylindrical lithium-ion battery module with variable contact surface," *Appl. Therm. Eng.*, vol. 123, pp. 1514–1522, 2017. <https://doi.org/10.1016/j.applthermaleng.2017.06.059> ↑7
- [31] Y. Huo, Z. Rao, X. Liu, and J. Zhao, "Investigation of power battery thermal management by using mini-channel cold plate," *Energy Convers. Manage.*, vol. 89, pp. 387–395, 2015. <https://doi.org/10.1016/j.enconman.2014.10.015> ↑7
- [32] A. Benabderrahmane, A. Benazza, S. Laouedj, and J. P. Solano, "Numerical analysis of compound heat transfer enhancement by single and two-phase models in parabolic trough solar receiver," *Mechanika*, vol. 23, pp. 55–61, 2017. <https://doi.org/10.5755/j01.mech.23.1.14053> ↑7

